Phytochemistry 70 (2009) 163–172

Contents lists available at ScienceDirect

Phytochemistry

journal homepage: www.elsevier.com/locate/phytochem

Cloning and expression analysis of a wood-associated xylosidase gene (*PtaBXL1*) in poplar tension wood

Raphael Decou [a], Sabine Lhernould [a], Françoise Laurans [b], Elodie Sulpice [a], Jean-Charles Leplé [b], Annabelle Déjardin [b], Gilles Pilate [b], Guy Costa [a,*]

[a] *Laboratoire de Chimie des Substances Naturelles, Groupe de Glycobiologie Forestière, Faculté des Sciences et Techniques, 123, Avenue Albert Thomas, 87060 Limoges, Cédex, France*
[b] *Unité Amélioration Génétique et Physiologie Forestière, INRA Orléans, BP 20619 Ardon, 45 166 Olivet, Cédex, France*

ARTICLE INFO

Article history:
Received 23 June 2008
Received in revised form 15 December 2008
Available online 21 January 2009

Keywords:
Poplar
Xylan
β-Xylosidase
Tension wood
Trees

ABSTRACT

In stems of woody angiosperms responding to mechanical stress, imposed for instance by tilting the stem or formation of a branch, tension wood (TW) forms above the affected part, while anatomically distinct opposite wood (OW) forms below it. In poplar TW the S3 layer of the secondary walls is substituted by a "gelatinous layer" that is almost entirely composed of cellulose and has much lower hemicellulose contents than unstressed wood. However, changes in xylan contents (the predominant hemicelluloses), their interactions with other wall components and the mechanisms involved in TW formation have been little studied. Therefore, in the study reported here we determined the structure and distribution of xylans, cloned the genes encoding the xylan remodeling enzymes β-xylosidases (PtaBXLi), and examined their expression patterns during tension wood, normal wood and opposite wood xylogenesis in poplar. We confirm that poplar wood xylans are substituted solely by 4-*O*-methylglucuronic acid in both TW and OW. However, although glucuronoxylans are strongly represented in both primary and secondary layers of OW, no 4-*O*-methylGlcA xylan was found in G-layers of TW. Four full-length *BXL* cDNAs encoding putative β-xylosidases were cloned. One, *PtaBXL1*, for which xylosidase activity was confirmed by heterologous expression in *Escherichia coli*, exhibited a wood-specific expression pattern in TW. In conclusion, xylan as *PtaBXL1*, encoding β4-xylosidase activity, are down-regulated in TW.

1. Introduction

Wood may appear to be a simple material, but its structure is quite complex. It consists largely of vessel elements and xylem fibers, with walls composed of three types of organic polymers: cellulose, hemicelluloses and lignin (Larson, 1994; Mellerowicz et al., 2001). In addition to endogenous developmental programs, a number of environmental factors, notably wind and asymmetric growth, may induce *de novo* wood formation. In poplar trees, tension wood (TW) appears at the upper face of inclined stems or branches (Timell, 1969), characterized by reduced proportions of vessel elements, and it is often formed more quickly than normal wood. In addition, a thick layer, named the gelatinous layer or G-layer is characteristically deposited in the secondary cell walls of TW. The principal characteristics of the secondary wall of gelatinous fiber cells are: (i) high cellulose contents (Roland et al., 1995); (ii) small amounts of phenolics, mainly G units (Joseleau et al., 2004) and (iii) cellulose microfibrils oriented largely parallel to the longitudinal axis of the cell (Wang et al., 2001). While the two main types of polymers, cellulose and lignin, have been intensively studied, little is known about the hemicelluloses, which provide a polysaccharidic matrix, forming links between each other and with cellulose microfibrils. The three major hemicellulosic components of wood are xyloglucans, glucomannans and xylans (Costa et al., 2002). Xyloglucans are hetero-polymers with repeated structures of different monosaccharides. The units identified to date are a heptasaccharide and a nonasaccharide; the first composed of four residues of β(1,4)-Glc and three terminal Xyl (XXXG) residues, linked to a main glucose chain by α(1,6) links (Edelmann and Fry, 1992), while the nonasaccharide consists of the heptasaccharide plus a Fuc residue α(1,2)-linked to Gal with a β(1,2) linkage to Xyl (XXFG). Glucomannans consist of chains of β(1,4)-Glc and β(1,4)-Man without any regularity in their sequences. Those that contain a single Gal residue in the side chains in a proportion similar to that of Glc are called galactoglucomannans.

Xylans are the major component of hemicelluloses in secondary cell walls, and thus in wood tissue (Kulkarni et al., 1999). They contain a main chain composed of Xyl residues linked by β(1,4) linkages. In woody plants xylose is substituted by units of α(1,2)

Abbreviations: BXL, β-xylosidase; TW, tension wood; OW, opposite wood; NW, normal wood.

* Corresponding author. Tel.: +33 555 45 72 16; fax: +33 555 45 77 65.
E-mail address: guy.costa@unilim.fr (G. Costa).

0031-9422/$ - see front matter © 2008 Elsevier Ltd. All rights reserved.
doi:10.1016/j.phytochem.2008.12.019

glucuronic acid or methylglucuronic acid, and the resulting polymers are known as glucuronoxylans (GX) (Aspinall, 1980; Ebringerova and Heinze, 2000). In birch (*Betula verrucosa*) and spruce (*Picea abies*) wood, xylan contains another sugar, e.g. α(1,2) galacturonic acid or α(1,3) rhamnose, forming xylo-oligosaccharides at their reducing ends (Shimizu et al., 1976; Johansson and Samuelson, 1977; Andersson et al., 1983). In various hardwood trees, e.g., aspen, beech and birch, some of the hemicellulose fraction consists of *O*-acetyl-(4-*O*-methyl-glucurono)xylan (Timell, 1969), in which the β(1, 4)-linked D-xylopyranosyl backbone is substituted with an α(1,2)-linked 4-*O*-methyl-D-glucuronic acid at approximately one in ten of the xylopyranosyl residues, which are also partially acetylated (Timell, 1969). The degree of acetylation in native aspen glucuronoxylan has been reported to be between 0.6 and 0.7 (Khan et al., 1990; Teleman et al., 2000). The function of acetylation in native glucuronoxylan is not clear and its effects on the wood's material properties are not well documented. However, the acetyl groups play a major role in the organization of lignified cell walls since they can cross-link with lignin (Hatfield et al., 1999) and interact with cellulose (Awano et al., 2002).

Our understanding of xylan biosynthesis and subsequent modification is still very incomplete, although the processes are known to involve numerous glycosyltransferases (Costa et al., 2002; Porchia et al., 2002; Lee et al., 2007a,b; Pena et al., 2007) and glycosylhydrolases (Coughlan and Hazlewood, 1993; Cosgrove, 1997; Prade, 1996; Kulkarni et al., 1999; Zeng et al., 2008). Notably: the partial purification of a xylan arabinosyltransferase from wheat has been reported (Porchia et al., 2002); a glycosyltransferase from Arabidopsis, IRX9, has been demonstrated to be required for normal xylan xylosyltransferase activity and normal elongation of the xylan chain (Pena et al., 2007); and three other glycosyltransferases from Arabidopsis – FRA8 (Zhong et al., 2005; Zhou et al., 2006), IRX8 (Persson et al., 2007; Pena et al., 2007) and PARVUS (Lee et al., 2007b) – have been shown to be required for the biosynthesis of the tetrasaccharide primer sequence (β-D-Xyl-(1,4)- β-D-Xyl-(1,3)-α-L-Rha(1,2)-α-D-GalA-(1,4)-D-Xyl) at the reducing end of glucuronoxylans.

It is also known that xylans may be hydrolyzed during plant cell wall maturation (Rahman et al., 2003; Tuncer and Ball, 2003), and several enzymes, including β(1,4)-endoxylanase, β-D-xylosidase, α-L-arabinofuranosidase, α-D-glucuronidase, acetylxylan esterase, and phenolic acid esterase have implicated roles in xylem remodeling (Sunna and Antranikian, 1997). Endo-β(1,4)-xylanases hydrolyze the insoluble xylan backbone into soluble xylo-oligosaccharides, while β-D-xylosidases hydrolyze xylo-oligosaccharides and xylobioses from their non-reducing ends (Sunna and Antranikian, 1997). Endoxylanases have been identified in several higher plants (Slade et al., 1989; Banik et al., 1997; Caspers et al., 2001; Suzuki et al., 2002), while β-D-xylosidases from a variety of bacteria, fungi (Sunna and Antranikian, 1997) and even plants (Chinen et al., 1982; O'Neill et al., 1989; Tezuka et al., 1993; Cleemput et al., 1997) have been purified and partially characterized. Seven genes encoding putative β-D-xylosidases have also been isolated from *Arabidopsis thaliana* recently (Goujon et al., 2003; Minic et al., 2004). Two of these genes, *AtBXL1* and (to a lesser extent) *AtBXL4*, are reportedly specifically expressed in secondary cell wall tissue (Goujon et al., 2003). The cited authors suggest that the secondary wall is susceptible to loosening, like the primary wall, but β-xylosidases acting on xylans are the mediators of this adaptive cell wall process. Xylosidase could be involved in the organization and loosening of glucuronoxylans in the cell wall, thereby facilitating lignin polymerization in the polysaccharide matrix (Goujon et al., 2003).

Prompted by the studies of Goujon et al. (2003), we have investigated enzymes with β-D-xylosidase activity in poplar TW and OW. The main objectives of our work were to assess the hypotheses that wood formation is associated with the expression of specific β-D-xylosidases, that TW and/or OW formation is correlated with up- or down-regulation of wood-specific β-D-xylosidases and (if so) obtain data on the expression patterns of the enzymes in the secondary cell wall that could provide new insights into the roles of xylan remodeling and/or recycling during secondary cell wall maturation.

2. Results

2.1. Purification and characterization of poplar xylans

The molecular composition of xylans purified from normal (NW), tension and opposite wood obtained from two-year-old poplar plants was analyzed by gas chromatography (GC) and mass spectrometry, and the results are summarized in Table 1. The sugar content of the purified fraction from the NW (1.5 g of sugar from 10 g of DW wood) consisted mainly of Xyl residues (84 mol%), 4-*O*-methylGlcA (12 mol%) and trace amounts of other monosaccharides. The oligosaccharide mass spectra acquired confirm that poplar wood xylans are hetero-polymers of 4-*O*-methyl-glucuronoxylan (Fig. 1A and B). The corresponding TW and OW extracts contained even higher proportions of xylan (92.9 and 90.5%, respectively) and no significant differences in sugar composition were observed between them (Table 1). The amount of xylan in TW (463 mg of sugar from 10 g of DW wood) is lower than in OW (731 mg of sugar from 10 g of DW wood). The level of branching with 4-*O*-methylGlcA was substantially lower in the samples of both TW and OW than in the NW samples.

2.2. Immunocytolocalization of the xylan epitopes in poplar stem tissues

AX1 antibodies raised against arabinoxylans (which recognize glucuronoxylans as well as arabinoxylans; Guillon et al., 2004) were used to localize xylans in TW and OW of stem sections collected from artificially tilted poplar trees. Strong labeling of the secondary cell walls of fibers, vessels and ray cells was observed (see light micrographs in Fig. 2A) in both TW and OW. The G-layer of the tension wood fibers was not labeled across the TW induction periods. No significant labeling was observed in control sections treated solely with the secondary antibody, confirming the specificity of the immunogold labeling. The labeling pattern in OW was similar to that observed in normal wood (data not shown).

Transmission electron microscopic observations confirmed that the labeling was strongest in the secondary cell wall layers, and no labeling was detected in the G-layer of tension wood fibers

Table 1
Sugar composition (mol%) of xylan-rich pools of the 4M KOH extracts from 2-year-old poplar trees. NW refers to wood from trees grown without tension for 2 years. For TW and OW, plants were grown for 1 year without tension followed by 1 year under tension. Sugars were trimethylsilylated before separation by GC.

Sugar	KOH extract (mol%)		
	NW	TW	OW
Rha	1.5	1	1.1
Fuc	0.2	_	_
Ara	0.8	_	0.6
Xyl	83.9	92.9	90.5
Man	0.4	_	0.3
Glc	0.5	0.9	0.6
Gal	0.9	_	0.7
GalA	_	1.3	1.3
GlcA	_	_	_
4-*O*-methylGlcA	12.2	4	4.9

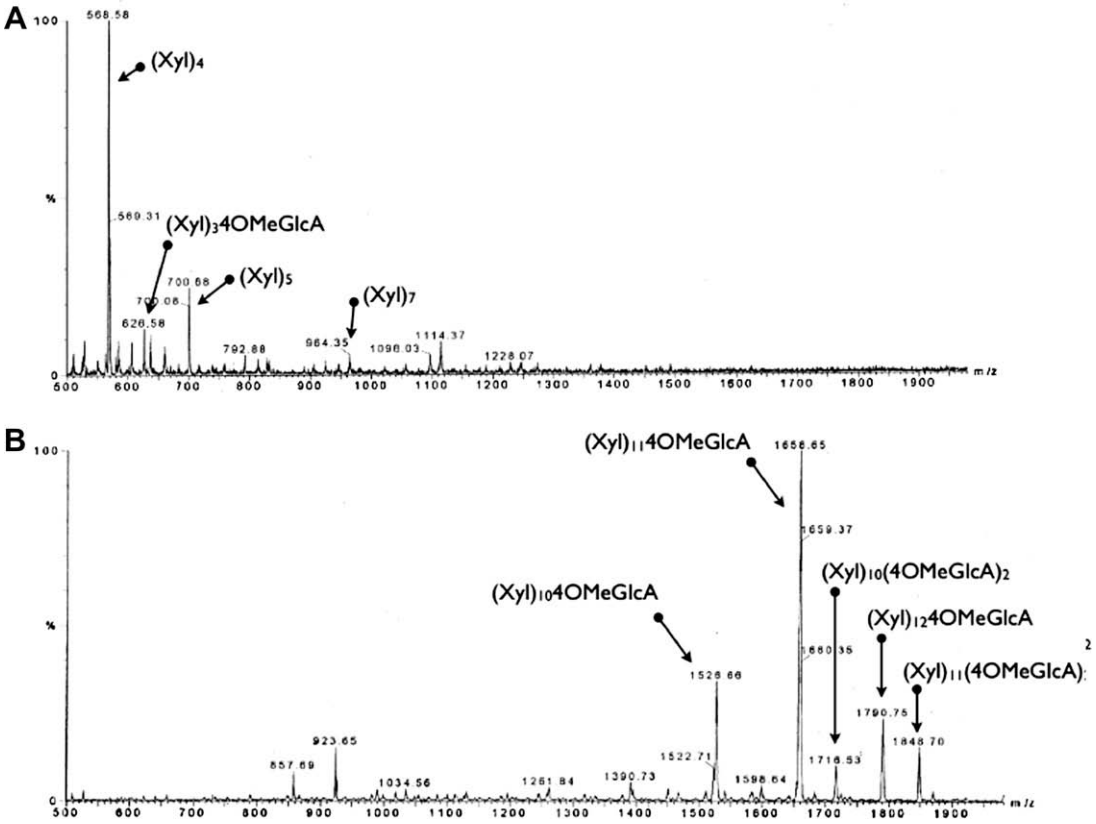

Fig. 1. Mass spectra of low molecular weight (A) and high molecular weight (B) xylan oligosaccharides separated by BioGel P4 chromatography after auto-hydrolysis of KOH extracts.

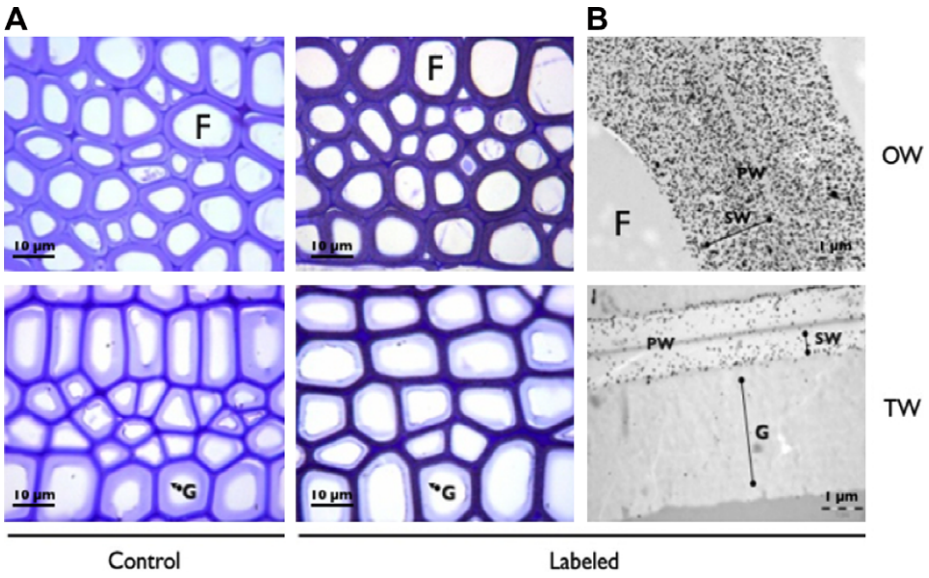

Fig. 2. (A) Light micrographs of opposite wood (OW) and tension wood (TW) labeled with and without monoclonal arabinoxylan antibodies (AX1). (B) Electron micrographs of wood secondary cell wall fibers from TW and OW labeled with AX1. PW, primary cell wall; SW, secondary cell wall; G, gelatinous layer.

(Fig. 2B). Interestingly, in tension wood fibers, which have thinner S2 layers than opposite wood, the AX1 labeling seemed to be concentrated at the interface between the S2 and G-layers. In contrast, the S2 layers from opposite wood fibers, which are thicker, exhibited uniform labeling. In both opposite and tension wood the primary cell wall and cell corner middle lamellae were also labeled, but to a lesser extent (data not shown).

2.3. Identification of poplar β-xylosidase-like genes (PtaBXLi)

Four poplar genes with high homology to genes known to encode β-xylosidases were isolated, and designated *PtaBXL1 2, 3* and *4*. Three were isolated from four wood EST libraries (Déjardin et al., 2004) – three containing sequences obtained from developing xylem (DX) samples (PTA-JXO0011, PTA-JXO1, and PTA-

JXT0013) and one of sequences from the cambial zone (CZ) (PTA-C0010) – while the other was cloned by a bio-informatic approach (http://genome.jgi-psf.org/). Whole poplar genome scanning demonstrated that their is only four distinct genes encoding putative β-xyloisdase enzyme while seven genes have been isolated from *A. thaliana* (Goujon et al., 2003). Three of them (*PtaBXL1, 2* and *3*) were subjected to RACE–PCR to determine corresponding full-length cDNAs (Table 2). The gene *PtaBXL1* is polyexonic, present in a single copy (*BamH*1 cutting) as shown in Fig. 3, and encodes a protein of 732 amino acids (MW 80.2 kDA, pI 8.64), with two predicted *N*-glycosylation sites (Fig. 4, Table 2). The other three genes (*PtaBXL2, 3* and *4*) encode proteins of 704, 757, and 704 amino acids (MW 75.8, 81.5 and 77.2; pI 5.19, 6.03 and 7.89, respectively), each harboring two to four potential *N*-glycosylation sites. PtaBXL1, 2 and 3 all have a predicted signal peptide at their N-termini, suggesting they have extra-cellular locations. PtaBXL4 was found to be targeted to the plasma membrane (Table 2). All the PtaBXLi proteins possess two consensus conserved domains corresponding to domains of the glucosyl-hydrolase three family (CAZy). A phylogenetic tree predicted from multiple alignment of translated peptidic sequences of PtaBXLi (PtaBXL1: AM117813; PtaBXL2 AM183258; PtaBXL3 AM183259 and PtaBXL4: AM183260) and AtBXLi (AtBXL1: BAB09906; AtBXL2: AAG10624; AtBXL3: BAB09531; AtBXL4: BAB11424, AtBXL5: BAB02547, AtBXL6: T49983 and AtBXL7: AAF17692) genes was generated (Fig. 5). PtaBXL1 and PtaBXL4 seem to be orthologous to AtBXL2 and AtBXL7, respectively. According to Fitch's definition (Fitch, 1970), poplar PtaBXL2 and PtaBXL3 are paralogous, and orthologous to the *A. thaliana* paralogs AtBXL3 and AtBXL4.

2.4. Heterologous activity of poplar PtaBXL1

PtaBXL1 cDNA was cloned into the pBAD expression vector (pBAD*PtaBXL1*), and the resulting construct was expressed in *Escherichia coli*. The recombinant protein, present in inclusion bodies, having a β-xylosidase activity was assayed *in vitro* with and without the artificial substrates pNPXyl, and pNPGlc, and with and without poplar xylan, birch xylan, and tamarin xyloglucan (negative control) oligosaccharides as substrates (Table 3). The recombinant *E. coli* enzyme PtaBXL1 hydrolyzed only substrates containing (1,4)-linked β-xylosyl residues. Thus, it appears to be a β-(1,4) xylosidase. In addition it hydrolyzed pNPXyl less efficiently than xylan oligosaccharides, suggesting that it is an exo-xylosidase that is most active towards polyxylosilated molecules.

2.5. Differential expression of poplar PtaBXL1

Northern blot analysis using total RNA from aspen developing xylem, cambium, leaves, roots and flower samples hybridized with *BXL1*, *BXL2*, *BXL3* and *BXL4* probes indicated that *PtaBXL1* is expressed specifically in the secondary-wall-enriched cambium and xylem (Fig. 6A, lanes 1 and 2), but not in the other examined organs, while the other three β-xylosidases – encoded by *PtaBXL2*, *PtaBXL3* and *PtaBXL4* – are not transcribed in xylem and cambium, but only in leaves, roots and flowers (Fig. 6A, lane 3, 4 and 5). *PtaBXL2* and *PtaBXL3* are expressed more strongly in leaves and roots than in flowers. Moreover, *PtaBXL3* seems to be more strongly transcribed than *PtaBXL2*, and *PtaBXL4* is the most weakly expressed poplar β-xylosidase. In order to substantiate these results, RT-PCR and RT-qPCR were conducted using *PtaBXLi*-specific primers and total RNA extracted from secondary-wall-enriched developing xylem as from leaves and roots tissues. A single band of 163 bp (Fig. 6B) was amplified from wood tissue samples, while no amplification products were obtained from leaf and root samples (Fig. 6C). In addition, cambium samples yielded an RT-PCR as RT-qPCR, product with weaker intensity than xylem samples, suggesting that *PtaBXL1* is most strongly expressed during second-

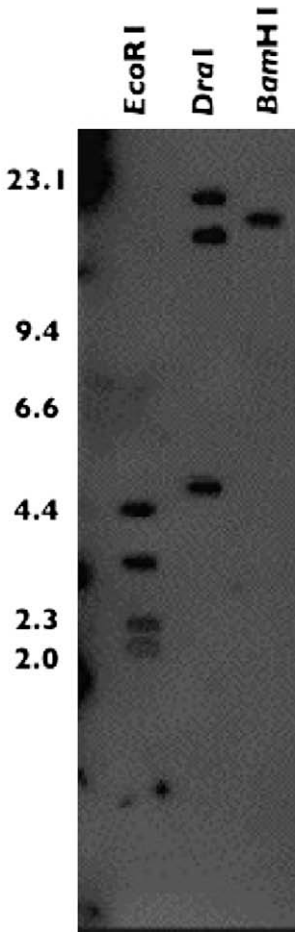

Fig. 3. Southern blot of poplar DNA digested with *EcoR*1, *BamH*1 and *Dra*1 hybridized with a partial 5′-end *PtaBXL1*-specific probe.

Table 2
Comparison of poplar genes encoding β(1,4)-xylosidase, the deduced proteins they encode, corresponding ORF lengths, numbers of exons, sizes of the proteins and their subcellular locations (predicted by SignalP and WoLF PSORT) and the number of *N*-glycosylation sites predicted by NetNGlyc.

	PtaBXL1	*PtaBXL2*	*PtaBXL3*	*PtaBXL4*
AC number	AM117813	AM183258	AM183259	AM183260
Gene length (bp)	3949	4213	4667	10,435
ORF length (bp)	2199	2115	2274	2115
Exon number	7	7	7	7
Protein length (aa)	732	704	757	704
N-glycosylation site (NetNGlyc)	^{123}N, ^{155}N	^{87}N, ^{328}N ^{456}N	^{365}N, ^{509}N	^{110}N, ^{263}N, ^{374}N, ^{396}N
Sub-cellular location (WoLF PSORT)	Extra-cellular	Extra-cellular	Extra-cellular	Plasma membrane
Peptide signal (SignalP)	21<SKA-LD>25	33<VSA-QS>38	33<VSA-QS>38	–

```
1          11         21         31         41         50
|          |          |          |          |          |
MPTSFIITLS VLFLGVSLQT SKALDPFACD PKDGTNRDLP FCQVNLPIHT
51         61         71         81         91        100
|          |          |          |          |          |
RVNDLIGRMT LQEKVGLLVN NAAAVPRLGI KGYEWWSEAL HGVSNVGPGT
101        111        121        131        141        150
|          |          | ▼        |          |          |
KFGGAFPVAT SFPQVITTAA SFNATLWEAI GRVVSDEARA MFNGGVAGLT
151        161        171        181        191        200
|  ▼       |          |          |          |          |
YWSPNVTYSV YPRWGRGQET PGEDPVVVGK YAASYVRGLQ GSDGIRLKVA
201        211        221        231        241        250
|          |          |          |          |          |
ACCKHFTAYD LDNWNGVDRF HFNAKVSKQD MVDTFDVPFR MCVKEGKVAS
251        261        271        281        291        300
|          |          |          |          |          |
VMCSYNQVNG IPTCADPNLL KKTVRGQWRL NGYIVSDCDS FGVYYGQQHF
301        311        321        331        341        350
|          |          |          |          |          |
TSPRRSSLGC YKAGLDLDCG PFLVTHRDAV KKAAEEAEIN NAWLKTLTFQ
351        361        371        381        391        400
|          |          |          |          |          |
ISLGIFDGSP LQAVGDVVPT MGPPTNQDLA VNAPKRLFIF KNRAFLLYSP
401        411        421        431        441        450
|          |          |          |          |          |
RHIFGPVALF KSLPFMLGNY EGLPCKYLFP LQGLAGFVSL LYLPGCSNVI
451        461        471        481        491        500
|          |          |          |          |          |
CAVADVGSAV DLAASADAVV LVVGADQSIE REGHDRVDFY LPGKQQELVT
501        511        521        531        541        550
|          |          |          |          |          |
RVAMAAKGPV LLVIMDLAIS GGGCSYNQVN GIPISDVCEG SSYRWPSFSN
551        561        571        581        591        600
|          |          |          |          |          |
CHGYMPWISY SRAIWETLRF TKVNWVPTWS WNKLHKFGSH HSKCTDDGFG
601        611        621        631        641        650
|          |          |          |          |          |
TPRRPPPWLR KCNHFQGRQS ELHMLDVIDS LLGMQVDVKN TGSMDGTHTL
651        661        671        681        691        700
|          |          |          |          |          |
LVYFRPPARH WAPHKQLVAF EKVHVAAGTQ QRVGINIHVC KSLSVVDGSG
701        711        721        731
|          |          |          |
IRRIPMGEHS LHIGDVKHSV SLQASILGVV ES
```

Fig. 4. Peptic sequence of *PtaBXL1*. The signal peptide in bold, *N*- and *C*-glycosylhydrolase three domains are underlined and *N*-glycosylation sites are marked with arrows.

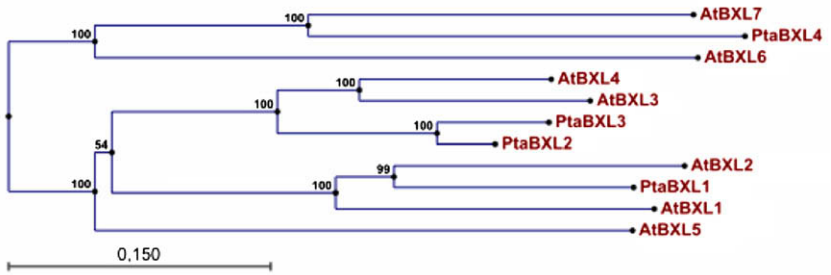

Fig. 5. Phylogenetic tree generated by the neighbor-joining method from an alignment of whole peptidic sequences deduced from seven *Arabidopsis thaliana* (AtBXL1, BAB09906; AtBXL2, AAG10624; AtBXL3, BAB09531; AtBXL4, BAB11424, AtBXL5, BAB02547, AtBXL6, T49983 and AtBXL7, AAF17692) and four poplar (PtaBXL1, AM117813; PtaBXL2, AM183258; PtaBXL3, AM183259 and PtaBXL4, AM183260) genes encoding β(1,4)-xylosidases. Numbers represent bootstrap support for relationships derived from DNA analyses.

Table 3
Specific activity of non-recombinant (pBAD) and recombinant PtaBXL1 from poplar (pBAD*PtaBXL1*) expressed in *E. coli* towards different substrates.

Substrate	Specific activity (nkat ml^{-1})	
	pBAD*PtaBXL1*	pBAD
*p*NP-β-D-Xylopyranoside[a]	9.2	0.94
*p*NP-β-D-Glucopyranoside[a]	0.56	0.48
Xylan from poplar wood[b]	19.4	0.21
Xylan from birch wood[b]	15.9	0.53
Xyloglucan from tamarin[b]	0.71	0.32

[a] pNP release from pNP-β-D-xylopyranoside or pNP-β-D-glucopyranoside was determined spectrophotometrically at 405 nm.

[b] Xyl releases from oligosaccharides were determined using a HPEAC system as described in Section 4. Activities were assayed in triplicate with 50 μg samples of proteins, and specific activities were expressed in katal, as the amount of enzyme needed to produce 1 mol of reducing sugar per second.

ary cell wall formation. The data also indicate that *PtaBXL1* is more weakly expressed in TW cambium than in OW cambium, although it is expressed at similar levels in TW and OW xylem (Fig. 6B and C). The internal control reaction yielded products of similar intensity and size, confirming that similar starting amounts of RNA were used in the RT-PCR and RT-qPCR experiments (Fig. 6B and C).

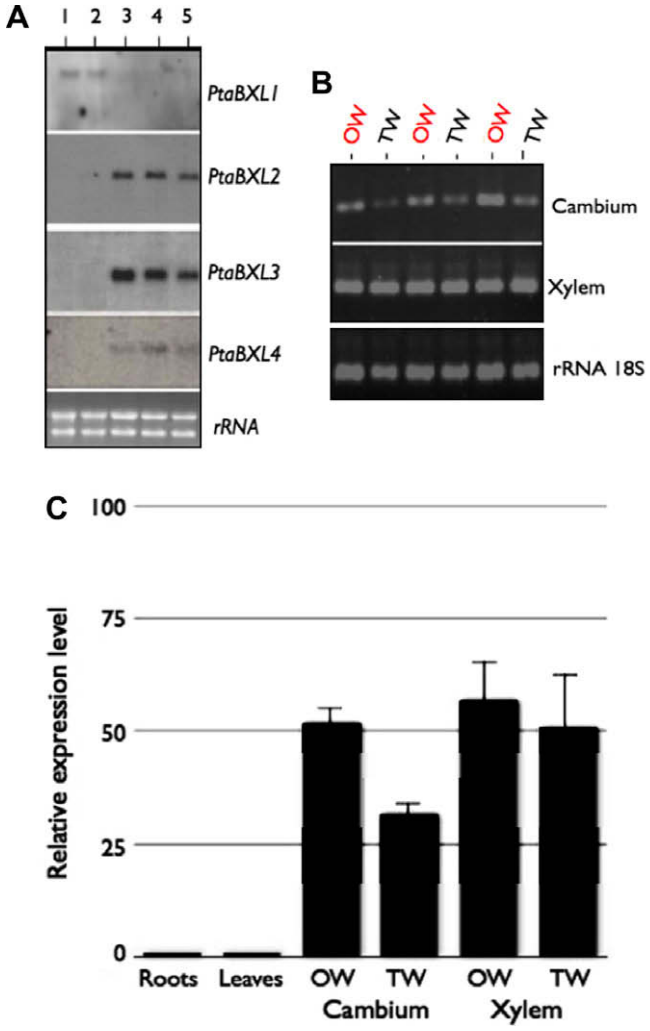

Fig. 6. (A) Northern blots of total RNA extracts from poplar clone 717-1B4 tissues (lanes 1–5: xylem, cambium, leaf, root and flower, respectively) probed with specific cDNAs corresponding to partial sequences of *PtaBXL1, PtaBXL2, PtaBXL3* and *PtaBXL4*. Ethidium bromide (rRNA) staining of RNA samples showing equal loading. (B) RT-PCR and (C) RT-qPCR analysis of *PtaBXL1* expression in opposite (OW) and tension wood (TW) from cambium and differentiated xylem and from leaf and root tissues. Total RNA was extracted from duplicate samples obtained from three different trees. Relative expression levels were calculated and the poplar 18S rRNA housekeeping gene was used as reference gene.

3. Discussion

Wood is essentially a mixture of fibers and vessel cells, both of which have secondary cell walls that are rich in cellulose and lignin (Mellerowicz et al., 2001; Besombes and Mazeau, 2005a,b; Pilate et al., 2004). In addition, they have hemicellulose components, which account for approximately 22% of the dry weight of normal poplar wood (Puls and Schuseil, 1993; Sun et al., 2001) and play important but poorly understood roles in the walls. We hypothesized that xylans – which have been described as being amongst the most important and abundant hemicellulosic polysaccharides (Puls and Schuseil, 1993; Kulkarni et al., 1999; Sun et al., 2001) – are extensively remodeled in secondary walls during certain wood formation processes, notably the formation of tension wood.

To assess the validity and implications of this hypothesis, we first characterized xylans in wood from our poplar model clone (INRA 717-1B4). We found that glucuronoxylans represent more than 92% of the hemicellulosic fraction, and the other 8% consists of glucomannans (3–6%) with, probably, a small proportion of xyloglucans (although it should be noted that solvents with a high concentration of alkali, such as the one used in our extraction protocol, generally extract xylans and glucomannans more efficiently than xyloglucans, which can interact more strongly with cellulose fibers and pectins). We also confirmed unambiguously that poplar wood is rich in 4-*O*-methyl-glucuronoxylan. In addition, GC and mass spectrometric analysis showed that the xylans in OW and TW have quite similar structures to those in normal wood. However, the xylan contents of NW, TW and OW differ significantly. Moreover, amounts of sugars appear to be lower in TW than in OW.

Assuming that the proportions of xylans and their branching levels may be positively correlated with the frequencies of cellulose cross-links (Suzuki et al., 2002; Zeng et al., 2008), their abundance in OW suggests that there is strong polymeric cohesion in this type of wood. In an attempt to find evidence of cross-linkage between xylans and lignin, we examined contributions from ferulics in the mass spectra obtained from our extracts, but found no support for the hypothesis proposed by Grabber et al. (2000, 2002) that ferulated xylans are able to bind to lignin (data not shown). Xylan acetylation is also known to increase frequencies of linkage between polysaccharides (Puls and Schuseil, 1993; Sun et al., 2001). However, the xylan extraction procedure with KOH we applied prevented us from quantifying the rates of their acetylation. Nevertheless, although we found no evidence for xylan linkage, we demonstrated that methyl-glucuronoxylans are abundant in the secondary cell walls of OW. We also showed that TW xylans are only located at the interface between the S2 and the G-layer, and not in the G-layer. Thus, the cell wall in the G-layer probably has low degrees of polysaccharide linkage, and hence low levels of cohesion and strength.

Remodeling of xylans during secondary cell wall formation implies the intervention of both xylan synthases – which have been studied as possible mediators of xylan maturation during secondary wall formation in French bean (Gregory et al., 2002; Zhou et al., 2007; Zeng et al., 2008) – and xylan hydrolases, which may modify nascent and/or embedded polysaccharides of the cell wall. Here we provide evidence of the involvement of β(1,4)-xylosidases (1,4-beta-D-xylan xylosylhydrolase EC 3.2.1.37), which are known to release D-xylopyranose from the non-reducing ends of the main chains of xylans. A large number of β(1,4)-xylosidases have been identified, but most of them originate from saprophytic bacteria

and fungi (Simpson et al., 2003). We found four β(1,4)-xylosidases in the poplar genome, cloned them and named them *PtaBXL1* (AM117813), *PtaBXL2* (AM183258), *PtaBXL3* (AM183259) and *PtaBXL4* (AM183260), which have high levels of homology to four of the seven *A. thaliana* β(1,4)-xylosidases previously described by Goujon et al. (2003) and Minic et al. (2004). *PtaBXLi* open reading frames have a similar size to those of all known plant β(1,4)-xylosidases (~2100 bp). All deduced proteins are addressed to the plasma membrane or the cell wall, and they all have at least at two sites for *N*-glycosylation. These findings are consistent with their putative extra-cellular location. The deduced amino acid sequences of all poplar genes (*PtaBXLi*) have been classified in the glycoside hydrolase family three (Henrissat, 1998). Arabidopsis, and barley β-D-xylosidases are grouped in this family, and share bi-functional activities, as both β-D-xylosidases and α-L-arabinofuranosidases (Lee et al., 2003; Minic et al., 2004). Poplar xylans are free of arabinofuranosyl residues, unlike the great majority of xylans found in herbaceous plants, so we did not investigate whether or not the poplar β-D-xylosidases have α-L-arabinofuranosidase activity and we cannot therefore exclude the possibility that they may have such activity.

After characterizing the genes encoding β(1,4)-xylosidases from poplar, we investigated their expression patterns in various plant tissues, with a particular focus on wood-forming cells. We found that only one (*PtaBXL1*) of the four poplar genes is specifically expressed in mature xylem. Moreover, blast analysis of *PtaBXL1* against nucleotide sequences from the *Populus* database (http://poppel.fysbot.umu.se) yielded good matches with three ESTs (A013P03; G086P11; G098P85) that were previously isolated from tension wood libraries. Interestingly, ESTs corresponding to *PtaBXL1* (Pta-JXO0011) have also been isolated from the poplar 717-1B4 tension wood library. During TW formation, *PtaBXL1* mRNAs are down-regulated in cambial zones whereas no differentially expression was detected in differentiating xylem.

Our data demonstrate that *PtaBXL1* encodes a wood-specific β(1,4)-xylosidase that is down-regulated during TW formation. In our model clone, 4-*O*-methyl-glucuronoxylan is strongly accumulated in OW and non-detectable in G-layer. Since the G-layer is implicated in stem bending, we hypothesize that OW is stronger than TW. Thus, the low amount of xylan in TW is probably correlated with its low strength, especially in the G-layer. Further, since xylans are probably heavily involved in interactions with lignins, the low amounts of lignin in the primary cell wall and between the S2 and G-layer of TW (Joseleau et al., 2004) may be causally correlated with the low amounts of xylans in these parts of the wood (present study). This would also reduce the strength of the secondary cell walls in TW, and enhance their capacity to deform, thereby facilitating stem bending. The presence of β-xylosidase would not be required for this process because of the low amounts of xylan and high plasticity of these cells.

In contrast, both xylans and lignin are abundant in the secondary cell walls of OW (Pilate et al., 2004). Hence, there are high possibilities for molecular interactions, cell wall cohesion should be strong, and the capacity for cell wall deformation weak in OW. Dynamic growth, during stem bending, implies continuous rearrangement of all the polymers. However, since cellulose and lignin cannot be readily modified, hemicellulosic components and their interactions with the two major polymers could play major roles during this process. It has been suggested that the length, and more probably the substitution level of glucuronoxylans, affect the degree of cross-linking with the lignin polymers (Lawako et al., 2005). Hence, modification of the network may change the woody properties of the secondary xylem and remodeling enzymes, such as β-xylosidases could reorganize the xylan cross-linkages with all the other polymers. If so, β-xylosidase may be essential for maintaining the plasticity of the cell wall during stem bending. However, other enzymes could also be involved in this remodeling process. For example, Zeng et al. (2008) have suggested that XETs act not only on xyloglucan but also probably on glucuronoarabinoxylan. Thus, the possible roles of XETs during the formation of tension wood also warrant attention.

4. Experimental

4.1. Plant material

Poplar trees of clone INRA 717-1B4 (*Populus tremula* × *P. alba*, section *Populus*) generated from micro-propagated shoots were transferred to a greenhouse, potted in compost (3 l) and individually supplied with water and fertilizers by a drip system. Shoots were artificially bent by tilting the pots at 45° from the vertical using a rigid sticks. Two months later, stems were harvested and samples from the cambial zone and differentiating xylem were collected from both the upper and lower sides of the stem, corresponding to tension wood (TW) and opposite wood (OW), respectively (Lafarguette et al., 2004). Normal wood (NW) plant refers to wood from other side identically treated plants were not tilted. The samples were then frozen in liquid nitrogen, stored at −80 °C and lyophilized before use.

4.2. Xylan extraction and characterization

Cell walls were obtained from the NW, TW and OW poplar wood samples then soluble sugars, pectins and hemicellulosic were sequentially extracted from them, as described by Moine et al. (2007). Lignins were removed from the acid-extracted residues by incubating them twice in acidic sodium chlorite (1.4 M) solution, pH 4, at 80 °C for 1 h and the recovered material was dialyzed against water. Xylans were partially purified from the hemicellulosic fraction by extraction with 4M KOH solution containing 3 mg ml^{-1} $NaBH_4$. Total carbohydrates were measured by the phenol sulfuric acid method (Dubois et al., 1956), and monosaccharides were determined after methanolysis (MeOH/HCl 0.5 N, 24 h, 80 °C) by gas–liquid chromatographic analysis of pertrimethylsilylated methylglycosides following the procedures of Kamerling et al. (1975), as modified by Montreuil et al. (1986).

Xylan rich-fractions from the samples were autohydrolyzed by incubation in distilled water for 40 h at 100 °C, as described by Cianca and Cerezo (1993). Oligosaccharides were then separated using a 10 × 480 mm BioGel P4 with water as the eluant and analyzed using a ZMD mass spectrometer (Micromass, UK) operating with the following settings: nebulization gas, 400 ml l^{-1}; ionization mode, electrospray positive ion; cone voltage, 30 V; acquisition time, 0.1 s per spray; inter spray delay, 0.05 s; acquisition mass range was from *m/z* 50 to 2000 uam.

4.3. DNA extraction and Southern blotting

Genomic DNA was extracted from 100 mg samples of leaves of plants cultured *in vitro* using a QIAGEN DNeasy plant mini kit® according to the manufacturer's instructions. The concentration and quality of the DNA in the samples were determined by nanospectrometry (NanoDrop ND1000, Labtech) following the manufacturer's recommendations.

Three μg of total genomic DNA were digested with one unit each of *Dra*1, *EcoR*1 and *BamH*1, separated on 0.8% (w/v) agarose gel in 0.5x Tris-borate buffer and transferred to a positively-charged Hybond-XL nylon membrane (Amersham Biosciences, UK) by passive blotting with 0.4 M NaOH. The immobilized DNA was then hybridized at 42 °C in a buffer containing 5 × SSC, 50% (v/v) deionized formamide, 50 mM sodium phosphate buffer (pH

7.0), 7.0% (w/v) SDS, 0.1% (w/v) *N*-lauryl sarcosine, 2.0% (w/v) blocking reagent (Roche, Germany) and a 163 bp digoxigenin (DIG)-labeled probe corresponding to a partial sequence of *Ptabxl1*, prepared by PCR amplification with SBXL1_fw and SBXL1_rv primers (Table 4). The hybridized membrane was washed with 2 × SSC and 0.1% (w/v) SDS for 20 min at room temperature and subsequently with 0.2 × SSC and 0.1% (w/v) SDS for 15 min at 65 °C. Chemiluminescent signals were detected on X-ray film (Lumi-film chemiluminescent Detection Film, Roche molecular) following the manufacturer's instructions.

4.4. RNA extraction, northern blotting and semi-quantitative reverse transcription-polymerase chain reaction (RT-PCR) analysis

The frozen wood material was ground to a fine powder in liquid nitrogen, and total RNA was extracted from 250 mg (fresh weight) samples of wood (TW or OW) using a QIAGEN RNeasy Plant mini kit® according to the manufacturer's instructions. The RNA concentration and quality of the samples were determined by nano-spectrometry (NanoDrop ND1000 Labtech) following the manufacturer's recommendations.

Total wood RNA (20 μg) was separated on a 0.7 M formaldehyde/1.2% (w/v) agarose gel in 1 × MOPS buffer (20 mM 3-(*N*-morpholino)propanesulfonic acid, 5 mM sodium acetate, 1 mM EDTA, pH 7.0) and transferred to a Hybond-XL membrane by capillary blotting with 10 × SSC. Hybridization, detection and Northern blot analyse were performed with the DIG-chemiluminescence system (see Section 4.3). The DIG-labeled probes, corresponding to partial sequences of *PtaBXL 1, 2, 3* and *4* are respectively named *BXL1* (163 bp), *BXL2* (209 bp), *BXL3* (170 bp), and *BXL4* (197 bp), and the sequences of their respective primers are presented in Table 4. Four independent Northern blot experiments were performed.

In each case, 2 μg of total RNA isolated as described above was reverse-transcribed using 500 ng of oligo(dT)12–18 and 200 units of SuperScript™ II RT in a total volume of 19 μl following the manufacturer's instructions (Invitrogen, Life technologies, USA). After first-strand cDNA synthesis, complementary RNAs to the cDNAs were removed by incubating the reaction mixture with 2 units (1 μl) of *E. coli* RNAse H at 37 °C for 20 min. PCR was then performed with pairs of primers corresponding to the partial sequences of *BXL1* (SBXL1_fw/SBXL1_rv), *BXL2* (SBXL2_fw/SBXL2_rv), *BXL3* (SBXL3_fw/SBXL3_rv) and *BXL4* (SBXL4_fw/SBXL4_rv) shown in Table 4. For quantitative PCR, the SYBR® Green I-based RT-qPCR was performed using the same set of oligonucleotide primers as above, in a 20 μl mix containing 10 μl of SYBR Green PCR Master Mix (ABI), 20 ng cDNA and 0.5 μM of each primer at the following conditions: 95 °C for 10 min, 40 cycles at 95 °C for 15 s and then at 60 °C for 1 min at 50 °C for 30 min, 95 °C for 15 min, and 45 cycles of 15 s at 95 °C and 1 min at 60 °C. RT-qPCR was performed with an ABI Prism7500 Sequence detector (Perkin–Elmer) in triplicates with standard deviations of threshold cycle (CT) values not exceeding 0.5. RT-PCR and RT-qPCR were calibrated with the amplicon of 18S ribosomal RNA molecule (NS51, 5′-GGGGGAGTATGGTCGCAAGGC-3′; NS61, 5′-TCAGTGTAGCGCGCGTGCGGC-3′).

Table 4
List of primers used for amplifying *PtaBXL1* (AM117813), *PtaBXL2* (AM183258), *PtaBXL3* (AM183259) and *PtaBXL4* (AM183260).

Primer	Sequence	Position
SBXL1_fw	5′-AGAGTAAATGACCTTATTGG-3′	151–171
SBXL1_rv	5′-TCCAATAGCCTCCCACAAAG-3′	294–314
SBXL2_fw	5′-AGGCCAGATCCTTCCAATGG-3′	1897–1917
SBXL2_rv	5′-CTGACAGGTCTGTTCAGAGG-3′	2086–2106
SBXL3_fw	5′-AACTAACTCAAGCACCTGG-3′	1885–1904
SBXL3_rv	5′-AAGAAAACTGTATGGCTTCC-3′	2035–2055
SBXL4_fw	5′-CTGAGAACTCAGAGACTCCTGG-3′	1759–1781
SBXL4_rv	5′-TCAGACTATAATAGTGACTGG-3′	1935–1956
3′BXL1-1	5′-TGGAGGGGTAGCTGGGCTCACC-3′	429–451
3′BXL1-2	5′-AGTCCAAACGTGACATATTCAG-3′	457–479
5′BXL2-1	5′-AACATTTGCAACTGCTGTTATCAAAAGTTGC-3′	1623–1654
5′BXL2-2	5′-GAAGAACGTCCACCCTGTCACGACTCTCTGC-3′	1579–1610
5′BXL3-1	5′-AGTCATTGGTACTTTGTCTACGTATGATTGTGG-3′	1705–1738
5′BXL3-2	5′-GGAACCAAAAATAATATCAGCTATGGCAGCTCC-3′	1647–1680
PtaBXL4_fw	5′-ATGGCGGGCAAGCATCCAGTTTTAC-3′	0–25
PtaBXL4_rv	5′-TCAGACTATAATAGTGACTGGGTGTTC-3′	2088–2115

4.5. Rapid amplification of cDNA ends (RACE) and PCR amplifications

To isolate full-length cDNAs corresponding to *PtaBXL1, 2* and *3*, we performed 5′- and 3′-RACE–PCR using a GeneRacer™ Advanced RACE Kit and primers listed in Table 4. 3′-RACE–PCR yielded the clone JXO0011, containing the 5′-UTR and 493 nucleotides after the initiator codon of *PtaBXL1*, while 5′-Full RACE–PCR yielded the clones JXT0013, including 502 nucleotides before the stop codon and the 3′ UTR of *PtaBXL2*, and C0010, including 571 nucleotides before the stop codon and the 3′ UTR of *PtaBXL3*. All the PCR reactions were performed in 50 μl mixtures with Platinum® Taq High Fidelity DNA Polymerase using a GeneAmp® 9700 PCR System (Applied Biosystems) following the protocol provided by Invitrogen. The sequence of *PtaBXL4* was identified from AGI (http://genome.jgi-psf.org/) by comparison with *A. thaliana* β-xylosidase genes, and PCR was applied to cDNA as described previously, with the forward and reverse primers PtaBXL4_fw and Ptabxl4r_rv, respectively (Table 4).

The PCR products were cloned into the pCR2.1-TOPO vector, using a TOPO TA Cloning® Kit and transformed into *E. coli* strain TOP10 following the manufacturer's instructions (Invitrogen One Shot® Cells) before DNA sequencing using an ABI PRISM Dye Terminator Cycle Sequencing Ready Reaction Kit with AmpliTaq DNA Polymerase and an 310 ABI PRISM sequencer (Amersham Biosciences, UK).

4.6. Heterologous expression of PtaBXL1

PtaBXL1 was sub-cloned in pBAD-TOPO (pBAD*PtaBXL1*), transformed TOP10 *E. coli* clones were grown in LB medium to mid-log phase (OD600 0.6–0.7), harvested by centrifugation (8000*g*, 10 min, 4 °C) and resuspended in 15 ml of 50 mM sodium phosphate buffer (pH 6.8) containing 0.1 mM DTT. The cells were then broken using an ultrasonic homogenizer (Labsonic U-Ultra 50, B. Braun, Germany) equipped with a 4 mm diameter, 127 mm long length titanium probe (40 T, Model 853 811/5) operating at 20 kHz. The resulting extract was centrifuged at 30,000*g*, 4 °C, for 30 min, and the supernatant (crude extract) was used for enzymatic assays. Protein concentrations of cell extracts were estimated by the Bradford dye binding assay (Bradford, 1976). Inclusion bodies were solubilized by 8 M urea in 20 mM sodium phosphate at pH 7.5. After centrifugation at 12,000*g* for 30 min to remove insoluble particulates, urea-denatured PtaBXL1 in solubilized lysate was refolded by stepwise dialysis against refolding buffer (100 mM NaCl, 100 mM Tris–HCl, pH 8.0, 2 mM dithiothreitol, 1% Chaps) to lower the urea concentration by 2 M at each step. β-xylosidase activities were determined spectrophometrically, in triplicate assays in which extracts were incubated in 50 mM sodium citrate buffer (pH 5.5) at 37 °C for 2 h with 5 mM of the chromophoric substrate *p*-nitrophenyl-β-D-xylopyranoside (pNPXyl) and *p*-nitrophenyl-β-D-glucopyranoside (pNPGlc), following the procedures described by La Grange et al. (1997) and Minic et al. (2004).

In addition xylose released from birch and poplar xylans, and tamarin xyloglucans, incubated with the protein extracts was measured using a DX500 high-performance liquid chromatography

system (Dionex, Sunnyvale) equipped with a 4 × 250 mm Carbopac PA-100 anion-exchange column, a Carbopac PA-100 guard column and an ED40 pulsed amperometric detector (mobile phase; 20–100 mM gradient of sodium acetate in 60 mM NaOH flow rate 1 ml min^{-1}). The acquired data were analyzed using the Dionex Peaknet software package.

4.7. Computer-based structural analysis

Sequence data were analyzed using the MacGDE software package, version 2.2 (Smith et al., 1994). Nucleotide and deduced amino acid sequences of the *PtaBXLi* genes were compared to those of genes/proteins compiled in the GenBank/DDBJ/EMBL databases using the BLAST program (Altschul et al., 1997). The putative functions of the PtaBXLi proteins were determined according to the similarity of their sequences to genes/proteins with known functions (*E* value cutoff = $1e^{-5}$), and their structural features were predicted from their isoelectric points (pI), molecular masses, hydrophobic/hydrophilic plots (Kyte and Doolittle, 1982) and secondary structure (Chou and Fasman, 1978) predicted using CLC free Workbench version 4.6.2. In addition, putative functional domains were found by searching the ScanPROSITE database (Gattiker et al., 2002).

4.8. Microscopy

Xylem samples collected from trees tilted to induce tension wood differentiation for 14 days, 28 days or 3 months (for details on tension wood formation, see e.g. Jourez et al., 2001) were microscopically examined. For this purpose, sections of about 5 mm were cut from tension and opposite wood samples and fixed for 4 h in 2.5% paraformaldehyde and 0.1% glutaraldehyde in 0.1 M McIlvaine citrate–phosphate buffer, pH 7.0. After dehydration in a graded series of ethanol, samples were embedded in medium grade LR White resin (London Resin Company Ltd., England). Semi-thin sections (1 μm thick) were collected using a diamond knife (Diatome) installed in an ultracut R microtome (Leica), placed on silanized slides (Dako Cytomation) and fixed by heating at 60 °C for 48 h. To prevent liquid evaporation, all subsequent incubations were conducted in a moist chamber. Sections were incubated for 1 h with a droplet of blocking solution containing 3% bovine serum albumin (BSA) and 0.05‰ Tween-20 in 10 mM Tris Buffered Saline (TBS) buffer, pH 7.5, and then 2 × 5 min with droplets of dilution buffer comprising 0.3% BSA and 0.05‰ Tween-20 in 10 mM TBS, pH 7.5. To label arabinoxylans the sections were incubated with the mouse AX1 monoclonal antibody (Guillon et al., 2004) in 1:150 dilution buffer, washed with TBS buffer, then incubated with 5 nm gold-conjugated goat anti-mouse serum (Amersham Biosciences, UK) in 1:50 dilution buffer. Control sections were obtained by omitting the AX1 primary antibody. Sections were post-stained with 1% Gentian Violet in water (Fluka, Sigma–Aldrich) and examined under a Leica DMR light microscope. Immunogold labeling was enhanced by a Silver Enhancing kit (British Biocell International, Cardiff, UK) according to the manufacturer's instructions.

Ultrastructural features of the various types of wood were observed using a Philips CM110 electron microscope operating at 80 KV to examine 70 nm thick sections from the resin blocks harvested on 200-mesh formvar-coated nickel grids and treated as follows. The grids were floated for 1 h in a blocking solution containing 3% bovine serum albumin (BSA) and 0.1‰ Tween-20 in 50 mM Tris Buffered Saline (TBS) buffer, pH 7.5, and then twice for 5 min in a dilution buffer containing 0.3% BSA and 0.1‰ Tween-20 in 50 mM TBS, pH 7.5. Arabinoxylans were labeled by floating the grids on drops of dilution buffer containing mouse AX1 monoclonal antibody (1:25), washing them in TBS buffer and incubating them with 5 nm gold-conjugated goat anti-mouse serum in 1:50 dilution buffer (Amersham Biosciences, UK). Control sections were obtained by omitting the AX1 primary antibody. The grids were subsequently floated for 25 min in 3% aqueous uranyl acetate solution to increase the contrast, and immunogold labeling was enhanced using a Silver Enhancing kit (British Biocell International, Cardiff, UK) according to the manufacturer's instructions.

References

Altschul, S.F., Madden, T.L., Schäffer, A.A., Zhang, J., Zhang, Z., Miller, W., Lipman, D.J., 1997. Gapped BLAST and PSI-BLAST: a generation of protein database search programs. Nucleic Acids Res. 25, 3389–3402.

Andersson, S.I., Samuelson, O., Ishihara, M., Shimizu, K., 1983. Structure of the reducing end-groups in spruce xylan. Carbohydr. Res. 111, 283–288.

Aspinall, G.O., 1980. Chemistry of cell wall polysaccharides. In: Preiss, J. (Ed.), The Biochemistry of Plants, vol. 3. Academic Press, London, pp. 473–500.

Awano, T., Takabe, K., Fujita, M., 2002. Xylan deposition on secondary cell wall of *Fagus crenata* fiber. Protoplasma 219, 106–115.

Banik, M., Li, C.D., Langridge, P., Fincher, G.B., 1997. Structure, hormonal regulation, and chromosomal location of genes encoding barley (1–4)-beta-xylan endohydrolases. Mol. Gen. Genet. 253, 599–608.

Besombes, S., Mazeau, K., 2005a. The cellulose/lignin assembly assessed by molecular modeling. Part 1: adsorption of a threo guaiacyl beta-*O*-4 dimer onto a beta cellulose whisker. Plant Physiol. Biochem. 43, 299–308.

Besombes, S., Mazeau, K., 2005b. The cellulose/lignin assembly assessed by molecular modeling. Part 2: seeking for evidence of organization of lignin molecules at the interface with cellulose. Plant Physiol. Biochem. 43, 277–286.

Bradford, M.M., 1976. A rapid and sensitive method for the quantification of microgram quantities of protein utilizing the principle of protein–dye binding. Anal. Biochem. 72, 248–254.

Caspers, M.P., Lok, F., Sinjorgo, K.M., van Zeijl, M.J., Nielsen, K.A., Cameron-Mills, V., 2001. Synthesis, processing and export of cytoplasmic endo-beta-1,4-xylanase from barley aleurone during germination. Plant J. 26, 191–204.

Chinen, I., Oouchi, K., Tamaki, H., Fukuda, N., 1982a. Purification and properties of thermostable beta-xylosidase from immature stalks of *Saccharum officinarum* L. (sugar cane). J. Biochem. 92, 1873–1881 (Tokyo).

Chou, P.Y., Fasman, G.D., 1978. Empirical predictions of protein conformations. Annu. Rev. Biochem. 47, 251–276.

Cianca, M., Cerezo, A.S., 1993. Autohydolysis of polysaccharides. Carbohydr. Res. Brazil 45, 54–61.

Cleemput, G., Hessing, M., Van Oort, M., Deconynck, M., Delcou, J.A., 1997. Purification and characterization of a β-D-xylosidase and an endo-xylanase from wheat flour. Plant Physiol. 113, 377–386.

Cosgrove, D.J., 1997. Assembly and enlargement of the primary cell wall in plants. Annu. Rev. Cell Dev. Biol. 13, 171–201.

Costa, G., Léonard, R., Lhernould, S., Carlué, M., Maftah, A., 2002. Plant glysosyltransferases: tool for plant glycosylation knowledges and biotechnology application. Recent Res. Dev. Plant Biol. 2, 103–120.

Coughlan, M.P., Hazlewood, G.P., 1993. Beta-1,4-D-xylan-degrading enzyme systems: biochemistry, molecular biology and applications. Biotechnol. Appl. Biochem. 17, 259–289.

Déjardin, A., Leplé, J.C., Lesage-Descauses, M.C., Costa, G., Pilate, G., 2004. Expressed sequence tags from poplar wood tissues – a comparative analysis from multiple libraries. Plant Biol. 6, 55–64.

Dubois, M., Gilles, K.A., Hamilton, J.K., Rebers, P.A., Smith, F., 1956. Colorimetric method for determination of sugars and related substances. Anal. Chem. 28, 350.

Ebringerova, A., Heinze, T., 2000. Naturally occurring xylans: structure, isolation procedures and properties. Macromol. Rapid Commun. 21, 542–556.

Edelmann, H.G., Fry, S.C., 1992. Effect of cellulose synthesis inhibition on growth and the integration of xyloglucan into pea internode cell walls. Plant Physiol. 100, 993–997.

Fitch, W.M., 1970. Distinguishing homologous from analogous proteins. Syst. Zool. 19, 99–113.

Gattiker, A., Gasteiger, E., Bairoch, A., 2002. ScanProsite: a reference implementation of a PROSITE scanning tool. Appl. Bioinformatics 1, 107–108.

Goujon, T., Minic, Z., El Amrani, A., Lerouxel, O., Aletti, E., Lapierre, C., Joseleau, J.P., Jouanin, L., 2003. AtBXL1, a higher plant (*Arabidopsis thaliana*) putative beta-xylosidase gene, is involved in secondary cell wall metabolism and plant development. Plant J. 33, 677–690.

Grabber, J.H., Ralph, J., Hatfield, R.D., 2000. Cross-linking of maize walls by ferulate dimerization and incorporation into lignin. J. Agric. Food Chem. 48, 6106–6113.

Grabber, J.H., Ralph, J., Hatfield, R.D., 2002. Model studies of ferulate–coniferyl alcohol cross-product formation in primary maize walls: implications for lignification in grasses. J. Agric. Food Chem. 50, 6008–6016.

Gregory, A.C., Smith, C., Kerry, M.E., Wheatley, E.R., Bolwell, G.P., 2002. Comparative subcellular immunolocation of polypeptides associated with xylan and callose synthases in French bean (*Phaseolus vulgaris*) during secondary wall formation. Phytochemistry 59, 249–259.

Guillon, F., Tranquet, O., Quillien, L., Utille, J.P., Ordaz Ortiz, J.J., Saulnier, L., 2004. Generation of polyclonal and monoclonal antibodies against arabinoxylans and their use for immunocytochemical location of arabinoxylans in cell walls of endosperm of wheat. J. Cereal Sci. 40, 167–182.

Hatfield, R.D., Grabber, J., Ralph, J., Brei, K., 1999. Using the acetyl bromide assay to determine lignin concentrations in herbaceous plants: some cautionary notes. J. Agric. Food Chem. 47, 628–632.

Henrissat, B., 1998. Glycosidase families. Biochem. Soc. Trans. 26, 153–156.

Johansson, M.H., Samuelson, O., 1977. Reducing end-groups in birch xylan and their alkaline degradation. Wood Sci. Technol. 11, 251–263.

Joseleau, J.P., Imai, T., Kuroda, K., Ruel, K., 2004. Detection *in situ* and characterization of lignin in the G-layer of tension wood fibres of *Populus deltoides*. Planta 219, 338–345.

Jourez, B., Riboux, A., Leclercq, A., 2001. Comparison of basic density and longitudinal shrinkage in tension wood and opposite wood in young stems of *Populus euramericana* cv Ghoy when subjected to gravitational stimulus. Can. J. Forest Res. 31, 1676–1683.

Kamerling, J.P., Gerwig, G.J., Vliegenhart, J.F.G., Clamp, J.R., 1975. Characterization by gas liquid chromatography mass spectrometry of pertrimethylsilyl glycosides obtained in methanolysis of glycoproteins and glycolipids. Biochem. J. 151, 491–495.

Khan, A.W., Lamb, K.A., Overend, P., 1990. Comparison of natural hemicellulose and chemically acetylated xylan as substrates for the determination of acetyl-xylan esterase activity in *Aspergilli*. Enzyme Microb. Technol. 12, 127–131.

Kulkarni, N., Shendye, A., Rao, M., 1999. Molecular and biotechnological aspects of xylanases. FEMS Microbiol. Rev. 23, 411–456.

Kyte, J., Doolittle, R., 1982. A simple method for displaying the hydropathic character of a protein. J. Mol. Biol. 157, 105–132.

La Grange, D.C., Pretorius, I.S., van Zyl, W.H., 1997. Cloning of the *Bacillus pumilus* beta-xylosidase gene (xynB) and its expression in *Saccharomyces cerevisiae*. Appl. Microbiol. Biotechnol. 47, 262–266.

Lafarguette, F., Leplé, J.C., Déjardin, A., Laurans, F., Costa, C., Lesage-Descauses, M.C., Pilate, G., 2004. Poplar genes encoding fasciclin-like arabinogalactan proteins are highly expressed in tension wood. New Phytol. 164, 107–121.

Larson, P.R., 1994. The Vascular Cambium. Springer-Verlag, Berlin.

Lawako, M., Henriksson, G., Gellerstedt, G., 2005. Structural differences between the lignin–carbohydrate complexes present in wood and in chemical pupls. Biomacromolecules 6, 3467–3473.

Lee, R.C., Hrmova, M., Burton, R.A., Lahnstein, J., Fincher, G.B., 2003. Bifunctional family 3 glycoside hydrolases from barley with α-L-arabinofuranosidase and β-D-xylosidase activity. J. Biol. Chem. 278, 5377–5387.

Lee, C., O'Neill, M.A., Tsumuraya, Y., Darvill, A.G., Ye, Z.H., 2007a. The irregular xylem9 mutant is deficiënt in xylan xylosyltransferase activity. Plant Cell Physiol. 48, 1624–1634.

Lee, C., Zhong, R., Richardson, E.A., Himmelsbach, D.S., McPhail, B.T., Ye, Z.H., 2007b. The PARVUS gene is expressed in cells undergoing secondary wall thickening and is essential for glucuronoxylan biosynthesis. Plant Cell Physiol. 48, 1659–1672.

Mellerowicz, E.J., Baucher, M., Sundberg, B., Boerjan, W., 2001. Unravelling cell wall formation in the woody dicot stem. Plant Mol. Biol. 1–2, 239–274.

Minic, Z., Rihouey, C., Do, C.T., Lerouge, P., Jouanin, L., 2004. Purification and characterization of enzymes exhibiting beta-D-xylosidase activities in stem tissues of Arabidopsis. Plant Physiol. 135, 867–878.

Moine, C., Krausz, P., Chaleix, V., Sainte-Catherine, O., Kraemer, M., Gloaguen, V., 2007. Structural characterization and cytotoxic properties of a 4-*O*-methylglucuronoxylan from *Castanea sativa*. J. Nat. Prod. 70, 60–66.

Montreuil, J., Bouquelet, S., Debray, H., Fournet, B., Spik, G., Strecker, G., 1986. Glycoproteins. In: Chaplin, M.F., Kennedy, J.F. (Eds.), Carbohydrate Analysis: A Practical Approach. IRL Press, Oxford, pp. 143–204.

O'Neill, R.A., Albersheim, P., Darvill, A.G., 1989. Purification and characterization of a xyloglucan oligosaccharide-specific xylosidase from pea seedlings. J. Biol. Chem. 264, 20430–20437.

Pena, M.J., Zhong, R., Zhou, G.K., Richardson, E.A., O'Neill, M.A., Darvill, A.G., York, W.S., Ye, Z.H., 2007. Arabidopsis irregular xylem8 and irregular xylem9: implications for the complexity of glucuronoxylan biosynthesis. Plant Cell 19, 549–563.

Persson, S., Caffall, K.H., Freshour, G., Hilley, M.T., Bauer, S., Pointdexter, P., Hahn, M.G., Mohnen, D., Somerville, C., 2007. The Arabidopsis irregular xylem8 mutant is deficient in glucuronoxylan and homogalacturononan, which are essential for secondary cell wall integrity. Plant Cell 19, 237–255.

Pilate, G., Chabbert, B., Cathala, B., Yoshinaga, A., Leple, J.C., Laurans, F., Lapierre, C., Ruel, K., 2004. Lignification and tension wood. C.R. Biol. 9–10, 889–901.

Porchia, A.C., Sorensen, S.O., Scheller, H.V., 2002. Arabinoxylan biosynthesis in wheat. Characterization of arabinosyltransferase activity in golgi membranes. Plant Physiol. 130, 432–441.

Prade, R.A., 1996. Xylanases: from biology to biotechnology. Biotechnol. Genet. Eng. Rev. 13, 101–131.

Puls, J., Schuseil, J., 1993. Chemistry of hemicelluloses: relationship between hemicellulose structure and enzymes required for hydrolysis. In: Coughlan, M.P., Hazlewood, G.P. (Eds.), Hemicelluloses and Hemicellulases. Portland Press, London, pp. 4–5.

Rahman, A.K., Sugitani, N., Hatsu, M., Takamizawa, K., 2003. A role of xylanase, α-L-arabinofuranosidase, and xylosidase in xylan degradation. Can. J. Microbiol. 49, 58–64.

Roland, J.C., Mosiniak, M., Roland, D., 1995. Dynamique du positionnement de la cellulose dans les parois des fibres textiles du lin (*Linum usitatissimum*). Acta Bot. Gallica 142, 463–484.

Shimizu, K., Ishihara, M., Ishihara, T., 1976. Hemicellulases of brown rotting fungus, *Tyromyces palustris*. II. The oligosaccharides from the hydrolysate of a hardwood xylan by the intracellular xylanase. Mokuzai Gakkaishi 22, 618–625.

Simpson, D.J., Fincher, G.B., Huang, A.H.C., Cameron-Mills, V., 2003. Structure and function of cereal and related higher plant (1->4)-beta-xylan endohydrolases. J. Cereal Sci. 37, 111–127.

Slade, A.M., Hoj, P.B., Morrice, N.A., Fincher, G.B., 1989. Purification and characterization of three (1–4)-beta-D-xylan endohydrolases from germinated barley. Eur. J. Biochem. 185, 533–539.

Smith, S.W., Overbeek, R., Woese, C.R., Gilbert, W., Gillevet, P.M., 1994. The genetic data environment an expandable GUI for multiple sequence analysis. Comput. Appl. Biosci. 10, 671–675.

Sun, R.C., Fanga, J.M., Tomkinsona, J., Gengb, Z.C., Liub, J.C., 2001. Fractional isolation, physico-chemical characterization and homogeneous esterification of hemicelluloses from fast-growing poplar wood. Carbohydr. Pol. 44, 29–39.

Sunna, A., Antranikian, G., 1997. Xylanolytic enzymes from fungi and bacteria. Crit. Rev. Biotechnol. 17, 39–67.

Suzuki, M., Kato, A., Nagata, N., Komeda, Y., 2002. A xylanase, AtXyn1, is predominantly expressed in vascular bundles, and four putative xylanase genes were identified in the *Arabidopsis thaliana* genome. Plant Cell Physiol. 43, 759–767.

Teleman, A., Lundqvist, J., Tjerneld, F., Stalbrand, H., Dahlman, O., 2000. Characterization of acetylated 4-*O*-methylglucuronoxylan isolated from aspen employing ^{1}H and ^{13}C NMR spectroscopy. Carbohydr. Res. 329, 807–815.

Tezuka, K., Hayashi, M., Ishihara, H., Nishimura, M., Onozaki, K., Takahashi, N., 1993. Purification and substrate specificity of beta-xylosidase from sycamore cell (*Acer pseudoplatanus* L.): application for structural analysis of xylose-containing *N*-linked oligosaccharides. Anal. Biochem. 211, 205–209.

Timell, T.E., 1969. The chemical composition of tension wood. Svensk Papperstidn 72, 173–181.

Tuncer, M., Ball, A.S., 2003. Co-operative actions and degradation analysis of purified xylose-degrading enzymes from *Thermonospora fusca* BD25 on spelt xylan. J. Appl. Microbiol. 94, 1030–1105.

Wang, H.H., Drummont, J.G., Reath, S.M., Hunt, K., Watson, P.A., 2001. An improved fibril angle measurement method for wood fibres. Wood Sci. Technol. 34, 493–503.

Zeng, W., Chatterjee, M., Faik, A., 2008. UDP-xylose stimulated glucuronyltransferase activity in wheat (*Triticum aestivum* L.) microsomal membranes: characterization and role in glucurono(arabino)xylan biosynthesis. Plant Physiol. 147, 78–91.

Zhong, R., Pena, M.J., Zhou, G.K., Nairn, Wood-Jones, A., Richardson, E.A., Morisson, W.H., Darvill, A.G., York, W.S., Ye, Z.H., 2005. Arabidopsis fragile fiber8, which encodes a putative glucuronyltransferase, is essential for normal secondary wall synthesis. Plant Cell 17, 3390–3408.

Zhou, G.K., Zhong, R., Richardson, E.A., Morrison, W.H., Nairn, C.J., Wood-Jones, A., Ye, Z.H., 2006. The poplar glycosyltransferase GT47C is functionally conserved with Arabidopsis fragile fiber8. Plant Cell Physiol. 47, 1229–1240.

Zhou, G.K., Zhong, R., Richardson, E.A., Himmelsbach, D.S., McPhail, B.T., Ye, Z.H., 2007. Molecular characterization of PoGT8D and PoGT43B, two secondary wall-associated glycosyltransferases in poplar. Plant Cell Physiol. 48, 689–699.